NJC

PAPER

View Article Online
View Journal | View Issue



Cite this: *New J. Chem.*, 2014, **38**, 5975

# Stereoselectivity through a network of non-classical CH weak interactions: a prospective study of a bicyclic organocatalytic scaffold†

Jens H. Aasheim,[a] Heike Fliegl,[b] Einar Uggerud,[b] Tore Bonge-Hansen*[a] and Odile Eisenstein*[bc]

Received (in Porto Alegre, Brazil) 28th August 2014,
Accepted 25th September 2014

DOI: 10.1039/c4nj01460j

www.rsc.org/njc

A prospective novel organocatalyst scaffold has been investigated by computational studies for its potential to induce stereoselective reactions. Density functional theory calculations (DFT) of an organocatalysed Diels–Alder reaction between cinnamaldehyde and cyclopentadiene, show that it is possible to induce selectivity by placing appropriate chemical groups on the scaffold. In the present case small substituents with strong electronic effects are found to be more effective in controlling the stereochemical induction than sterically bulky substituents. We show, using noncovalent interaction analysis (NCI plots), that the $CF_3$ group is especially efficient in improving the stereochemical control as well as increasing the reaction rate.

## Introduction

Since organocatalysis re-emerged more than 10 years ago, it has established itself as a fast moving field of research as described in several reviews.[1] The use of small organic molecules to catalyze reactions has proven to be a practical and efficient way of preserving atom economy and achieving good yields and high enantioselectivity in many catalytic asymmetric transformations. New reactions and novel catalysts are constantly being added to the organocatalytic arsenal, increasing its usefulness and scope. Since the seminal report by MacMillan *et al.* of the first highly enantioselective Diels–Alder reaction of cyclopentadiene and α,β-unsaturated aldehydes in 2000,[2] there has been numerous accounts of organocatalysed cycloaddition reactions.[3] Many of them show a preference for the *exo* product.[4] Since then the MacMillan group has developed a series of efficient and useful imidazolidinone organocatalysts, capable of catalyzing a wide range of reactions by means of iminium ion catalysis.[5] In addition to MacMillan, Jørgensen–Hayashi diarylprolinol silyl ether catalysts[6] and List's proline catalyzed reactions[7] have shown the large potential of iminium/enamine organocatalysis.

One of the first studies of organocatalysis was carried out by MacMillan who used MM3 Monte Carlo calculations.[2] Following this study, computational chemistry, has been considered as a helpful tool in both describing, explaining and also validating organocatalytic structures, selectivity and mechanisms. Additional relevant and notable examples are by the groups of Houk[8] and Tomkinson.[9] It is thus attractive to consider the possibility of using computational methods to go beyond rationalization and envisage the prediction and rational catalyst design as shown for example by Tomkinson,[9] Houk,[10] Moitessier[11] and also one of us.[12] One essential aspect of organocatalysis is the representation of the weak interactions that exist between the various groups of the reactants. This requires the use of a methodology that properly represents dispersion forces. The group of Truhlar has been especially active in this field, and has developed several levels of the Minnesota functional that is appropriate for these kinds of studies.[13] Among the various functionals of this family, M06-2X, parameterized for chemical species without metal atoms, is well adapted for applications involving main group thermochemistry, kinetics and non covalent interactions.[13b] It has been used successfully for studying organocatalytic and cycloaddition reactions.[14,15] This functional has been selected for the present study.

The main purpose of this work is to study the possibility of reactivity manipulation, by creating a synthetically viable organocatalytic system that includes adjustable electronic and steric effects. The core of the system is a rigid bicyclic structure, to limit the degrees of freedom and thus provide a better control of the conformational space in addition to significantly simplifying

[a] *Department of Chemistry, University of Oslo, PO Box 1033, Blindern, 0315 Oslo, Norway. E-mail: tore.hansen@kjemi.uio.no; Fax: +47 228 55441; Tel: +47 228 55446*
[b] *Centre for Theoretical and Computational Chemistry (CTCC), Department of Chemistry, University of Oslo, P. O. Box 1033, Blindern, 0315 Oslo, Norway*
[c] *Institut Charles Gerhardt, UMR 5253 CNRS Université Montpellier 2, cc1501, Place E., Bataillon, 34095 Montpellier, France. E-mail: odile.eisenstein@univ-montp2.fr; Fax: +33 467144839; Tel: +33 467143306*

† Electronic supplementary information (ESI) available: Cartesian coordinates of all reported structures as well as the total electronic and zero-point energies. See DOI: 10.1039/c4nj01460j

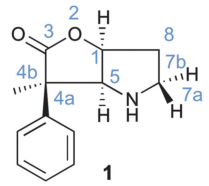


1

Fig. 1 Bicyclic lactone (BL) used as organocatalyst.

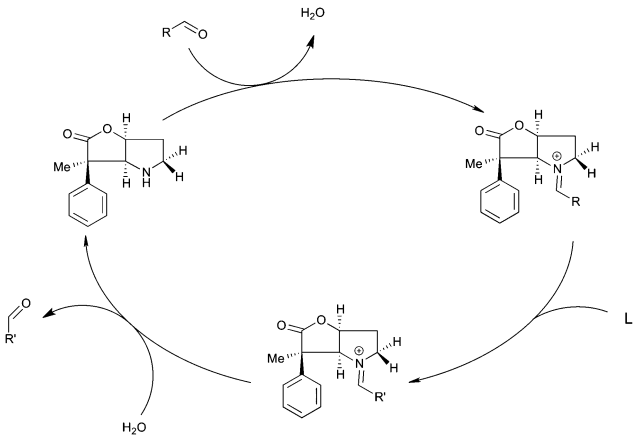


Scheme 1 The catalytic cycle, involving the condensation of the imine and an activated carbonyl.

the calculations. Conformational control will also provide a means to shield one side of the reactive site, hence yielding stereochemical control.

A possibly interesting system is the bicyclic Geissman–Waiss lactone (BL) (Fig. 1) as a candidate for this exploratory study. This lactone provides a bicyclic skeleton with a $sp^2$-hybridised carbonyl,[16] providing the needed structural rigidity. The reaction that is considered is shown in Scheme 1. The amine group is transformed into an iminium through a condensation reaction. Then, the reaction between the iminium carrying the reactive group R and the substrate (reaction between R and L giving R′) occurs in a chiral environment that could induce stereocontrol, which can be further influenced by the nature of the group at the 4 position of the lactone. Hydrolysis of the iminium liberates the end product and regenerates the amine form of BL, which re-enters the catalytic cycle.

With these basic structural elements in place we would have a tunable system that could be modified relatively easy by changing the aromatic shielding group. The reaction that we consider is a Diels–Alder reaction in which the iminium is conjugated to a C=C double bond that serves as a dienophile.

## Computational procedure

All structures were computed using the hybrid functional M06-2X[13] and the def2-TZVP[17] basis set for all atoms. All calculations were performed with the Gaussian 09 computational software package.[18] Visualizations were done with the beta version of CYLview.[19] Transition states and energy minima were characterized by analytical calculations of harmonic frequencies. IRC-calculations were performed to confirm the connection of transition structures to reactants and products. In these bimolecular reactions, the transition states connects to an adduct between the two reactants. The most stable form of this adduct (obtained from the IRC calculations) serves as origin of energy for calculating the Gibbs energy profiles for each set of reactants. We report Gibbs energies calculated in gas phase for $T$ = 298 K and $p$ = 1 atm. The network of weak interactions was identified using the Non Covalent Interaction (NCI) approach.[20] The analysis was carried out with the NCIplot software,[21a] with VMD[21b] as visual interface. These methods have been used to identify weak interactions in a wide variety of chemical and biochemical systems, and for discussing asymmetric induction.[22]

## Results and discussion

The basic reaction considered is the Diels–Alder reaction between cinnamaldehyde and cyclopentadiene (CP) as shown in Scheme 2, referred to as the uncatalyzed reaction. The lowest set of transition states are shown in Fig. 2, while higher transition states related to other conformations of the cinnamaldehyde are disregarded because they will not contribute significantly to products.

In accordance with other theoretical studies of the Diels–Alder reaction,[8e,23] all transition states correspond to an asynchronous concerted reaction pathway.

The two new carbon–carbon bond lengths differ by about 0.2 Å for both the *endo* and the *exo* reactions, as shown in Fig. 2. The calculations show a slight preference for the *exo* reaction, in contrast to the normal *endo* preference usually attributed to secondary orbital interactions between the incoming CP and the carbonyl group.[24] A possible reason for this difference is the presence of additional secondary interactions between the incoming CP and the π-system of the phenyl ring in the *exo* reaction.

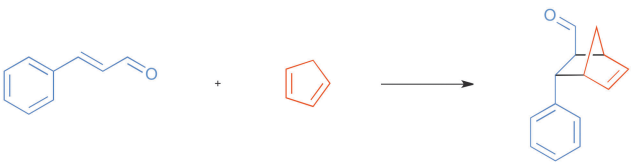


Scheme 2 Uncatalyzed Diels–Alder reaction.

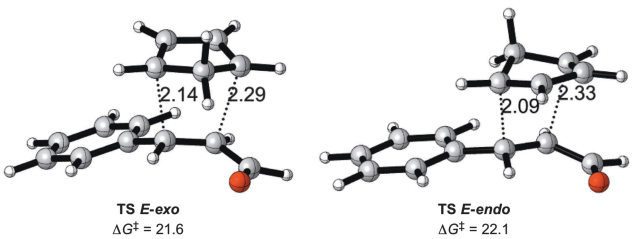


Fig. 2 Transition states for the uncatalyzed Diels–Alder reaction with Gibbs energies of activation in kcal $mol^{-1}$ relative to the adduct formed by cyclopentadiene and cinnamaldehyde, and selected distances in Å.

 

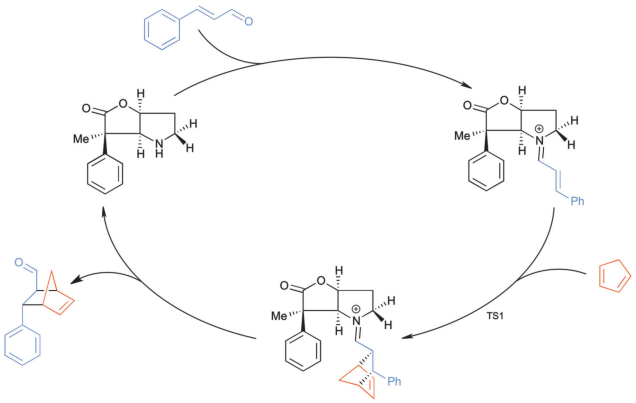


Scheme 3 The catalytic cycle of the organocatalysed Diels–Alder reaction between CP and the *E*-isomer of the iminium ion formed from cinnamaldehyde and BL.

The catalysed version of the reaction, following the proposal presented in Scheme 1, is shown in Scheme 3. The condensation of the cinnamaldehyde and the bicyclic lactone (BL) catalyst yields the conjugated iminium ion (Scheme 2), which can serve as an activated dienophile in the Diels–Alder reaction. Hydrolysis recovers the carbonyl group, in the product, and the amine functionality of BL. This study focuses on the cycloaddition step, as it is the rate determining step of the catalytic cycle.[9c]

To induce stereoselectivity in Diels–Alder reactions (Scheme 3) one needs to control three aspects: (i) the formation of the *E*- or *Z*-iminium ion isomer; (ii) *endo*- or *exo*-attack; (iii) attack on either side of the iminium ion, which will be referred to as top and bottom.

The condensation reaction between cinnamaldehyde and the bicyclic lactone (BL) catalyst (**1**) forms an iminium ion with either an *E* (H on imine carbon cisoid to the lactone) or a *Z* conformation. The calculations show a preference of 2 kcal mol$^{-1}$ for the **1-*E*** over the **1-*Z*** isomer, indicating that the condensation is conformationally controlled at the C=N double bond period (Fig. 3). The reason for this slight energy preference is likely to come from the close proximity of the phenyl ring at C4 of the lactone (see Fig. 1 for labelling) and the π system of the imimium moiety in the *Z*-conformation. It remains to be determined if this preference for the *E* over *Z* isomer translates into the transition states, and contributes to differentiate the top from bottom faces of the iminium and the *endo* from the *exo* pathways.

Fig. 4 displays the preferred transition states TS1 for the Diels–Alder reaction between the **1-*E*** iminium ion and CP. They all correspond to asynchronous concerted reactions and have activation barriers that are of similar magnitude to that of the uncatalyzed reaction (Fig. 2). The Gibbs energies of activation are the differences in Gibbs energies of the transition state and of the most stable adduct formed between **1-*E*** and CP. The lowest transition state is only 2 kcal mol$^{-1}$ lower (19.2 *versus* 21.6 kcal mol$^{-1}$ for the catalyzed and uncatalyzed systems, respectively). Thus the iminium and the aldehyde forms of the activated dienophile have similar reactivities.

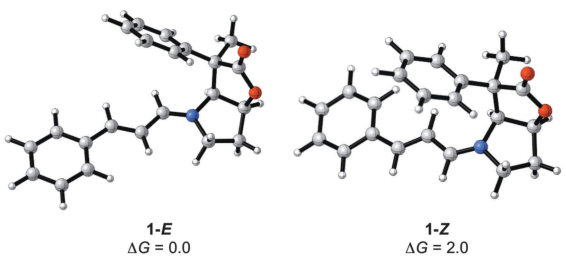


Fig. 3 *E*/*Z* iminium ions formed by the condensation of **1** and cinnamaldehyde with relative Gibbs energies in kcal mol$^{-1}$.

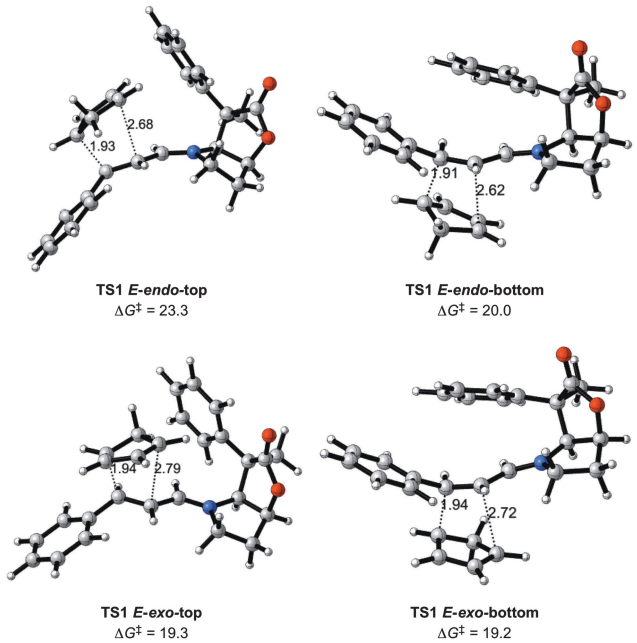


Fig. 4 Transition states for the reaction between CP and iminium ion **1-*E*** with Gibbs energies of activation in kcal mol$^{-1}$ and relevant distances in Å.

The *exo* attack is slightly preferred over the *endo* approach by 2 kcal mol$^{-1}$ on average. The preference for the *exo* attack is thus somewhat larger in the presence of BL (compare Fig. 2 and 4). Unfortunately, the *exo* attack is not associated with a significant differentiation for approach on one or another of the two faces. This is illustrated by a negligible difference in energy of only 0.1 kcal mol$^{-1}$ between the top and bottom transition states. In contrast, the *endo* attack differentiates between the two faces, and the bottom approach is preferred by 3.3 kcal mol$^{-1}$ over the top approach (Fig. 4). This indicates that the phenyl group is quite effective in directing the reaction towards one side of the iminium moiety for the *endo* attack, but unfortunately not for the preferred *exo* approach. This is due to the inherent flexibility of the iminium chain and some limited flexibility at the C4 phenyl group.

Before considering the effects of further modification of the BL catalysts, the following points have been established: (i) the BL-structure contributes to differentiate addition to the top and bottom faces for the *endo* transition states, but not sufficiently for the preferred *exo* transition states; (ii) the energy preference for the *E*- over *Z*-iminium ion isomer is conserved in the transition states; (iii) the *exo* attack of CP on the *E* isomer is preferred over the *endo* one. Finally, the catalyst has only a small impact on the rate of reaction since the activation

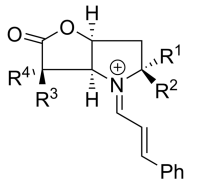

**1**: $R^1$ = H $R^2$ = H $R^3$ = Ph $R^4$ = Me
**2**: $R^1$ = H $R^2$ = H $R^3$ = m-xylene $R^4$ = Me
**3**: $R^1$ = H $R^2$ = H $R^3$ = tBu $R^4$ = Me
**4**: $R^1$ = H $R^2$ = Me $R^3$ = Ph $R^4$ = Me
**5**: $R^1$ = $CH_2OMe$ $R^2$ = H $R^3$ = Ph $R^4$ = Me
**6**: $R^1$ = H $R^2$ = H $R^3$ = p-F-Ph $R^4$ = Me
**7**: $R^1$ = H $R^2$ = H $R^3$ = Ph $R^4$ = F
**8**: $R^1$ = H $R^2$ = $CF_3$ $R^3$ = Ph $R^4$ = Me

Fig. 5 An overview of investigated catalysts **1–8**.

barriers are lowered by only 2 kcal $mol^{-1}$ compared to the uncatalyzed systems.

The next topic concerns the effect of substituents $R^1$, $R^2$, $R^3$ and $R^4$ (Fig. 5) on the activation energy and selectivity of the reaction (*endo vs. exo* and top *vs.* bottom). The Gibbs energies of the eight transition states relative to the most stable adduct formed between CP and each of the relevant iminium ions are given in Table 1. The associated *endo* : *exo* ratio and ee for both the *endo* and *exo* addition, obtained from a Boltzman analysis carried out at 298 K, is given in Table 2.

The results of Table 1 show that the Gibbs energies of activation for the Diels–Alder reaction vary between 15 and 25 kcal $mol^{-1}$, which indicates that the nature of the substituents influence the global rate of the reaction. An electron-withdrawing group close to the iminium moiety ($R^2$ = $CF_3$, entry 8) significantly lowers the energy of all transition states. This is consistent with the well-known accelerating effect of electron acceptor groups on the dienophile.[2,9,25] Interestingly, changing $R^3$ from Ph to *t*Bu (entry 3) also gives relatively low activation barriers, especially for the addition to the preferred *E*-isomer. In total, the influence of $R^3$ on the activation energy is relatively modest, indicating that the BL catalyst does not significantly affect the reaction rate.

Table 1 Gibbs energies of activation (kcal $mol^{-1}$), relative to the most stable adduct formed between cyclopentadiene and the relevant iminium ions, for the catalyzed Diels–Alder reaction. The transition state with the lowest energy in each system is in *italic*

| | Entry | TS-*endo*-top | TS-*endo*-bottom | TS-*exo*-top | TS-*exo*-bottom |
|---|---|---|---|---|---|
| 1 | **TS1-*E*** | 23.3 | 20.0 | 19.3 | *19.2* |
| | **TS1-*Z*** | 22.5 | 21.9 | 23.2 | 21.2 |
| 2 | **TS2-*E*** | 22.7 | 20.2 | 19.1 | *18.9* |
| | **TS2-*Z*** | 22.5 | 23.3 | 23.3 | 23.1 |
| 3 | **TS3-*E*** | 18.7 | 19.0 | *17.2* | 17.5 |
| | **TS3-*Z*** | 20.5 | 19.8 | 19.4 | 18.8 |
| 4 | **TS4-*E*** | 23.4 | 20.6 | *19.7* | 19.9 |
| | **TS4-*Z*** | 24.2 | 22.8 | 24.5 | 22.6 |
| 5 | **TS5-*E*** | 25.0 | 20.7 | 21.4 | 20.2 |
| | **TS5-*Z*** | 19.8 | 18.6 | 20.6 | *17.6* |
| 6 | **TS6-*E*** | 23.8 | 19.8 | 19.5 | *18.5* |
| | **TS6-*Z*** | 23.1 | 21.3 | 23.2 | 20.7 |
| 7 | **TS7-*E*** | 22.1 | 19.5 | 19.1 | *18.5* |
| | **TS7-*Z*** | 21.8 | 20.9 | 22.0 | 20.5 |
| 8 | **TS8-*E*** | 18.4 | 18.6 | *15.5* | 17.5 |
| | **TS8-*Z*** | 18.4 | 19.7 | 20.6 | 19.6 |

Table 2 *endo* : *exo* ratios and ee (%) for the *endo* and the *exo* reactions

| | *endo* : *exo* | ee – *endo* | ee – *exo* |
|---|---|---|---|
| **1** | 1 : 6.9 | 91.5 *S*,*S*[a] | 2.1 *S*,*S* |
| **2** | 1 : 17 | 96.1 *S*,*S* | 16.7 *S*,*S* |
| **3** | 1 : 13 | 26.7 *R*,*R* | 23.0 *R*,*R* |
| **4** | 1 : 7.9 | 94.0 *S*,*S* | 22.1 *R*,*R* |
| **5** | 1 : 4.9 | 71.2 *R*,*R* | 96.4 *R*,*R* |
| **6** | 1 : 9.5 | 86.7 *S*,*S* | 62.6 *S*,*S* |
| **7** | 1 : 6.3 | 82.6 *S*,*S* | 39.4 *S*,*S* |
| **8** | 1 : 54 | 22.6 *S*,*S* | 93.6 *R*,*R* |

[a] *S* and *R* refer to the absolute configuration at the two carbons of the dienophile.

Table 2 shows that the *exo* addition is always preferred, but the *endo* : *exo* ratio varies between 1 : 4.9 (entry 5) to 1 : 54 (entry 8). These two entries giving the lowest and highest *endo* : *exo* ratio, correspond to a $CH_3$ substituent at $R^2$ for entry 5 and $CF_3$ for entry 8. Since these two groups have similar effective vdW radii,[26] this indicates that other factors influence the selectivity. The significant lowering of the activation barriers with $CF_3$, and notably for the *exo* addition, could be responsible for this result. Changes in positions $R^3$ and $R^4$ have less influence on the *endo* : *exo* ratio. Even replacing Me with F at $R^4$ gives similar *endo* : *exo* ratio (entries 1 and 7). However, increasing the bulk of $R^4$, as for entry 2 with $R^4$ = *m*-xylene and entry 3 with $R^4$ = *t*Bu, gives larger *exo* : *endo* ratio than $R^4$ = phenyl.

Entry 1 is rather unique in giving such a small ee for the *exo* approach. For all other entries, the ee ratio is larger and can be even very large like for entries 5 and 8. The ee from the *endo* addition is always very large with the exception of entries 3 and 8. However, we do not need to discuss further the *endo* addition, as it is not preferred.

The most attractive case appears to be entry 8. The structure of the lowest transition state is given in Fig. 6. As mentioned earlier, this entry is associated with an increase in the reaction rate and a high *exo* selectivity, in addition to high enantiomeric selectivity. Lowering of the energy barrier is an expected result of the presence of an electron withdrawing group on the dienophile, as known in the Alder rule.[2,9,25] This does not however, account for the high selectivity in the *exo* addition and the significant preference for adding to the top face of the iminium ion. In order to obtain a deeper insight into this issue, an analysis of the noncovalent interactions was performed for the four *E* iminium ion transition states of entry 8 with NCIplot.[21]

Fig. 7 shows the result of the NCI analysis for the lowest transition state (**TS8-*E*-*exo*-top**) associated with entry 8. The weak interactions revealed by the NCI analysis are color coded from blue, for the strongest attractive weak interactions (hydrogen bonds, for example), to red for repulsive ones (steric clashes). In between, the very weak van der Waals interactions appear in green. Focus is mostly placed on the spaces that define the selectivity of the reaction. Fig. 7 shows that large green surfaces occur in the space between the incoming CP and both the $R^4$ phenyl group and the $R^2$ $CF_3$ group of BL. They are clearly associated with weak interaction between the CH bonds of CP and both the electron density of the phenyl ring and the

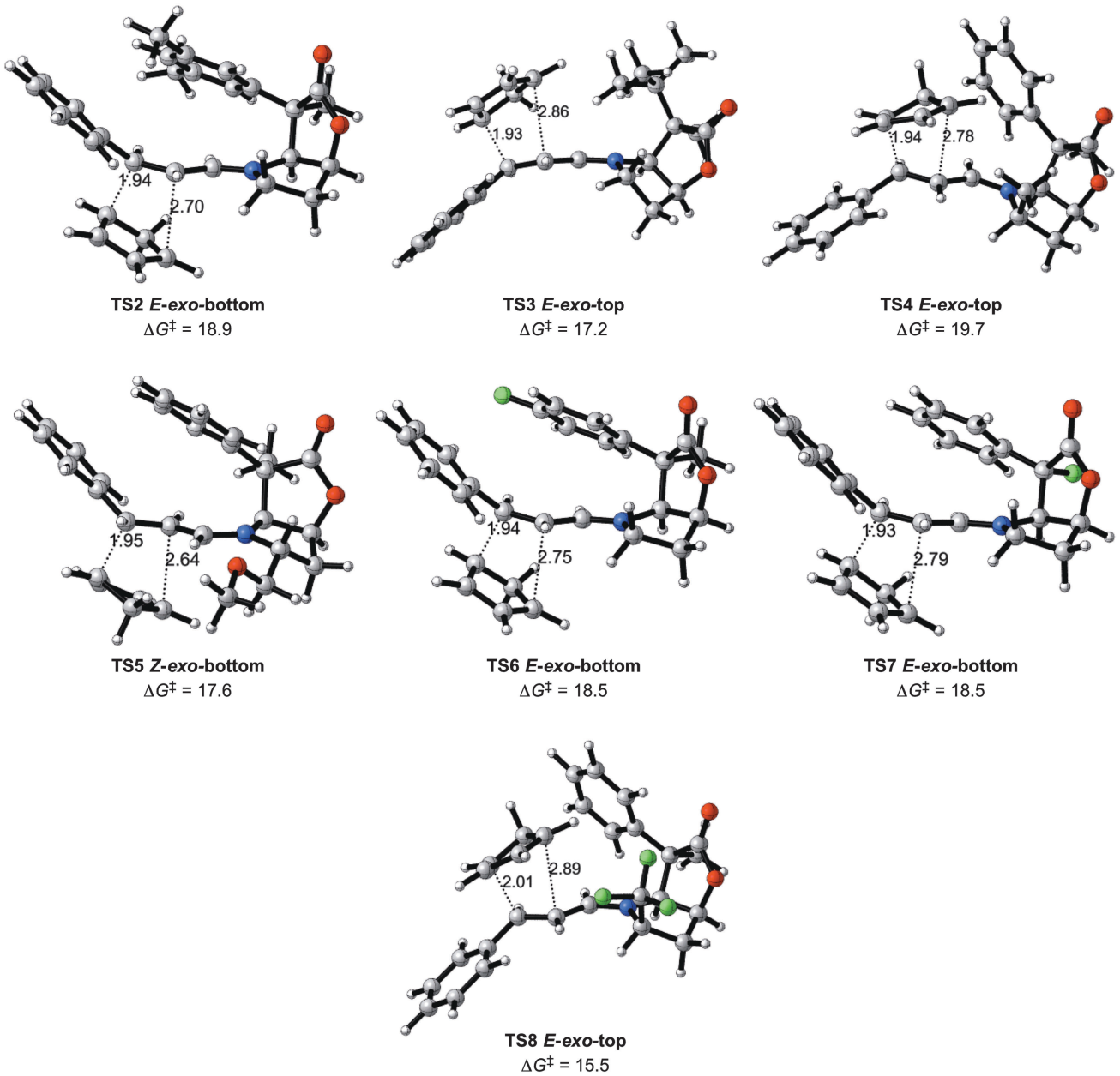


Fig. 6 The preferred transition states (**TS2** to **TS8**) for entries **2** to **8** (Table 1) with Gibbs energies of activation in kcal mol$^{-1}$, and selected distances in Å.

electron density at the fluorine atoms. These interactions are representative of non-classical CH···X interactions, whose importance in determining the structures of large systems have been established.[27] Unfortunately, there is not yet any quantitative relation between the size of the surface combined with its colour, and the energy of the interaction. However, a decrease of the size of the surface and a change of colour from darker to lighter green is indicative of a decrease in the magnitude of the weak interactions.

Thus, going to the less preferred transition states for entry 8 is associated with a decrease, or disappearance, of the green surfaces. In particular going from **TS8-*E-exo*-top** to **TS8-*E-endo*-top**, which corresponds to a raise of 2 kcal mol$^{-1}$, (Table 1), shows a clear decrease of the green surfaces between CP and the phenyl and $CF_3$ groups (Fig. 8). It seems that in the *exo* orientation, the CH bonds of CP creates the best network of dispersion interactions with the two electron rich groups. In the case of the bottom attacks, these weak interactions between CP and the phenyl and $CF_3$ groups are lost and the interaction between the $R^4$ phenyl group and the iminium skeleton does not fully compensate (Fig. 9).

The NCI analysis suggests the paradoxical result that it could be preferable to attack the iminium from the most hindered side because approach on this side is in fact dominated by weak interactions. One can thus understand the influence of the $CF_3$ group that modifies the electron distribution and increases the electron density in the appropriate part of the space and enhances the attractive interactions.

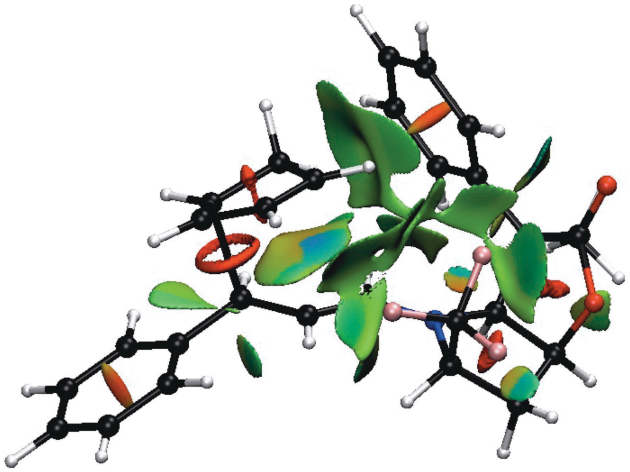

Fig. 7 Color-coded noncovalent interactions (NCI) surfaces (attractive decreasing from blue to green, repulsive increasing from yellow to red) for **TS8-*E*-*exo*-top**.

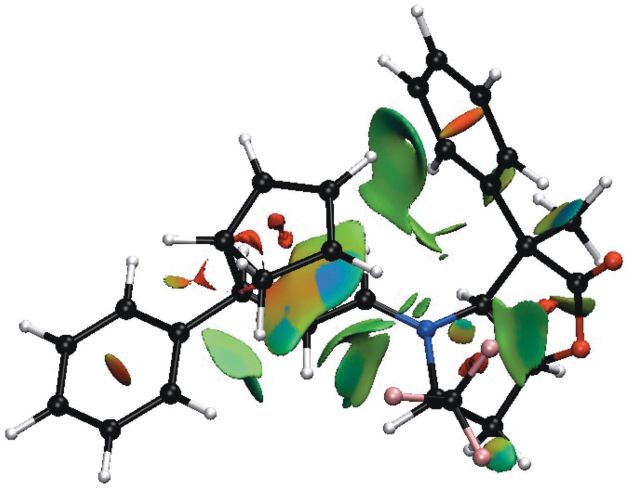

Fig. 8 Color-coded noncovalent interactions (NCI) surfaces (attractive decreasing from blue to green, repulsive increasing from yellow to red) for **TS8-*E*-*endo*-top**.

Proper substitutions on the BL catalyst (for example by introducing an electron withdrawing group such as $CF_3$) highlight the possibility to direct selectivity by creating an electronic environment that could fit the approaching reagent, an effect somewhat related to enzymatic control. The ideal system may have to be adapted to the reaction and even to the two substrates. This is not surprising in regard of the very high specificity of enzymatic catalysis.

## Conclusions

In this prospective study of an organized reaction, DFT calculations have been used to identify the parameters that control the stereocourse of the reaction. A Diels–Alder reaction between cinnamaldehyde and cyclopentadiene was used as a representative case because of the importance of this reaction in organic synthesis.

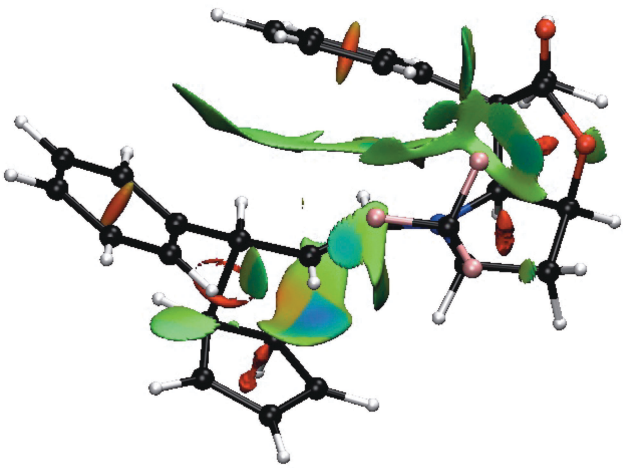

Fig. 9 Color-coded noncovalent interactions (NCI) surfaces (attractive decreasing from blue to green, repulsive increasing from yellow to red) for **TS8-*E*-*exo*-bottom**.

A bicyclic organic scaffold (BL) has been selected based on its relative rigidity, and because it possesses several sites that can be functionalized. DFT calculations and NCI plots for analysis were used to evaluate the steric and electronic effects of a series of modifications on BL, and their influence on the kinetics and stereochemical selectivity. An ideal catalyst should induce a high degree of stereochemical control and appropriately adjust reactivity to maximize the reaction yield without compromising the selectivity. In the presented case, the studies have shown that the shielding effects of appropriately positioned sterically bulky substituents (such as *t*Bu) are surpassed by smaller substituents exerting a strong electron withdrawing effect (such as $CF_3$). This EWG group lowers the energy barrier for all cycloadditions and especially that for the *exo* cycloaddition. Furthermore, the calculations show that the bicyclic scaffold is not as rigid as initially thought, which is one of the reasons of the limited impact of steric hindrance. This study shows that computations and analysis of the electronic structures along the reaction pathway can guide experiments and save chemical resources.

## Acknowledgements

J. H. A. thanks the Centre for Theoretical and Computational Chemistry (CTCC) and NOTUR for use of their computational resources. E. U., O. E. and H. F. thank for support by the Norwegian Research Council through the CoE for Theoretical and Computational Chemistry (Grant No. 179568/V30). This work has received support from the Norwegian Supercomputing Program (NOTUR) through a grant of computer time (Grants No. NN4654K). O. E. thanks the CTCC for an adjunct professorship position and the French CNRS and the MENESR for funding.

## Notes and references

1 (*a*) P. I. Dalko and L. Moisan, *Angew. Chem., Int. Ed.*, 2001, **40**, 3726; (*b*) P. I. Dalko and L. Moisan, *Angew. Chem., Int. Ed.*, 2004, **43**, 5138; (*c*) A. Dondoni and A. Massi,

 

*Angew. Chem., Int. Ed.*, 2008, **47**, 4638; (*d*) P. Melchiorre, M. Marigo, A. Carlone and G. Bartoli, *Angew. Chem., Int. Ed.*, 2008, **47**, 6138; (*e*) G. Lelais and D. W. C. MacMillan, *Aldrichimica Acta*, 2006, **39**, 78; (*f*) B. R. Buckley, M. C. Kimber and N. H. Slater, *Annu. Rep. Prog. Chem., Sect. B: Org. Chem.*, 2012, **108**, 98; (*g*) U. Scheffler and R. Mahrwald, *Chem. – Eur. J.*, 2013, **19**, 14346.

2 K. A. Ahrendt, C. J. Borths and D. W. C. MacMillan, *J. Am. Chem. Soc.*, 2000, **122**, 4243.

3 (*a*) B. F. Bonini, E. Capitò, M. Comes-Franchini, M. Fochi, A. Ricci and B. Zwanenburg, *Tetrahedron: Asymmetry*, 2006, **17**, 3135; (*b*) R. M. Wilson, W. S. Jen and D. W. C. MacMillan, *J. Am. Chem. Soc.*, 2005, **127**, 11616; (*c*) M. Lemay and W. W. Ogilvie, *Org. Lett.*, 2005, **7**, 4141; (*d*) A. Erkkilae, I. Majander and P. M. Pihko, *Chem. Rev.*, 2007, **107**, 5416.

4 (*a*) T. Kano, Y. Tanaka and K. Maruoka, *Org. Lett.*, 2002, **8**, 2687; (*b*) J. B. Brazier, J. L. Cavill, R. L. Elliot, G. Evans, T. J. K. Gibbs, I. L. Jones, J. A. Platts and N. C. O. Tomkinson, *Tetrahedron*, 2009, **65**, 9961.

5 (*a*) J. F. Austin and D. W. C. MacMillan, *J. Am. Chem. Soc.*, 2002, **124**, 1172; (*b*) A. B. Northrup and D. W. C. MacMillan, *J. Am. Chem. Soc.*, 2002, **124**, 2458; (*c*) S. G. Ouellet, J. B. Tuttle and D. W. C. MacMillan, *J. Am. Chem. Soc.*, 2005, **127**, 32.

6 (*a*) M. Marigo, T. C. Wabnitz, D. Fielenbach and K. A. Jørgensen, *Angew. Chem., Int. Ed.*, 2005, **44**, 794; (*b*) K. Juhl and K. A. Jørgensen, *Angew. Chem., Int. Ed.*, 2003, **42**, 1498.

7 (*a*) B. List, *Acc. Chem. Res.*, 2004, **37**, 548; (*b*) B. List, R. A. Lerner and C. F. Barbas III, *J. Am. Chem. Soc.*, 2000, **122**, 2395; (*c*) B. List, *J. Am. Chem. Soc.*, 2000, **122**, 9336; (*d*) B. List, P. Pojarliev and J. Martin, *Org. Lett.*, 2001, **3**, 2423.

8 (*a*) S. Bahmanyar and K. N. Houk, *J. Am. Chem. Soc.*, 2001, **123**, 11273; (*b*) C. Allemann, R. Gordillo, F. R. Clemente, P. H.-Y. Cheong and K. N. Houk, *Acc. Chem. Res.*, 2004, **37**, 558; (*c*) F. R. Clemente and K. N. Houk, *Angew. Chem., Int. Ed.*, 2004, **43**, 5765; (*d*) R. Gordillo, J. Carter and K. N. Houk, *Adv. Synth. Catal.*, 2004, **346**, 1175; (*e*) R. Gordillo and K. N. Houk, *J. Am. Chem. Soc.*, 2006, **128**, 3543; (*f*) V. Guner, K. S. Khuong, A. G. Leach, P. S. Lee, M. D. Bartberger and K. N. Houk, *J. Phys. Chem. A*, 2003, **107**, 11445.

9 (*a*) J. L. Cavill, R. L. Elliott, G. Evans, I. L. Jones, J. A. Platts, A. M. Ruda and N. C. O. Tomkinson, *Tetrahedron*, 2006, **62**, 410; (*b*) G. J. S. Evans, K. White, J. A. Platts and N. C. O. Tomkinson, *Org. Biomol. Chem.*, 2006, **4**, 2616; (*c*) G. Evans, T. J. K. Gibbs, R. L. Jenkins, S. J. Coles, M. B. Hursthouse, J. A. Platts and N. C. O. Tomkinson, *Angew. Chem., Int. Ed.*, 2008, **47**, 2820.

10 K. N. Houk and P. H.-Y. Cheong, *Nature*, 2008, **455**, 309.

11 C. R. Corbeil, S. Thielges, J. A. Schwartzentruber and N. Moitessier, *Angew. Chem., Int. Ed.*, 2008, **47**, 2635.

12 M. Bruvoll, T. Hansen and E. Uggerud, *J. Phys. Org. Chem.*, 2007, 206.

13 (*a*) Y. Zhao and D. G. Truhlar, *Acc. Chem. Res.*, 2008, **41**, 157; (*b*) Y. Zhao and D. G. Truhlar, *Theor. Chem. Acc.*, 2008, **120**, 215.

14 T. A. Rokob, A. Hamza and I. Pápai, *Org. Lett.*, 2007, **9**, 4279.

15 S. Schenker, C. Schneider, S. B. Tsogoeva and T. Clark, *J. Chem. Theory Comput.*, 2011, **7**, 3586.

16 (*a*) A. Barco, N. Baricordi, S. Benetti, C. De Risi, G. P. Pollini and V. Zanirato, *Tetrahedron*, 2007, **63**, 4278; (*b*) A. G. H. Wee, *J. Org. Chem.*, 2001, **66**, 8513.

17 F. Weigend and R. Ahlrichs, *Phys. Chem. Chem. Phys.*, 2005, **7**, 3297.

18 M. J. Frisch, G. W. Trucks, H. B. Schlegel, G. E. Scuseria, M. A. Robb, J. R. Cheeseman, J. A. Montgomery Jr., T. Vreven, K. N. Kudin, J. C. Burant, J. M. Millam, S. S. Iyengar, J. Tomasi, V. Barone, B. Mennucci, M. Cossi, G. Scalmani, N. Rega, G. A. Petersson, H. Nakatsuji, M. Hada, M. Ehara, K. Toyota, R. Fukuda, J. Hasegawa, M. Ishida, T. Nakajima, Y. Honda, O. Kitao, H. Nakai, M. Klene, X. Li, J. E. Knox, H. P. Hratchian, J. B. Cross, V. Bakken, C. Adamo, J. Jaramillo, R. Gomperts, R. E. Stratmann, O. Yazyev, A. J. Austin, R. Cammi, C. Pomelli, J. W. Ochterski, P. Y. Ayala, K. Morokuma, G. A. Voth, P. Salvador, J. J. Dannenberg, V. G. Zakrzewski, S. Dapprich, A. D. Daniels, M. C. Strain, O. Farkas, D. K. Malick, A. D. Rabuck, K. Raghavachari, J. B. Foresman, J. V. Ortiz, Q. Cui, A. G. Baboul, S. Clifford, J. Cioslowski, B. B. Stefanov, G. Liu, A. Liashenko, P. Piskorz, I. Komaromi, R. L. Martin, D. J. Fox, T. Keith, M. A. Al-Laham, C. Y. Peng, A. Nanayakkara, M. Challacombe, P. M. W. Gill, B. Johnson, W. Chen, M. W. Wong, C. Gonzalez and J. A. Pople, *Gaussian 03, Revision B.04*, Gaussian, Inc., Wallingford, CT, 2004.

19 C. Y. Legault, *CYLview. version 1.0b*, Université de Sherbrooke, Canada, 2008.

20 E. R. Johnson, S. Keinan, P. Mori-Sanchez, J. Contreras-Garcia, A. J. Cohen and W. T. Yang, *J. Am. Chem. Soc.*, 2010, **132**, 6498.

21 (*a*) J. Contreras-Garcia, E. R. Johnson, S. Keinan, R. Chaudret, J.-P. Piquemal, D. N. Beratan and W. T. Yang, *J. Chem. Theory Comput.*, 2011, **7**, 625; (*b*) W. Humphrey, A. Dalke and K. Schulten, *J. Mol. Graphics*, 1996, **14**, 33, see also http://www.ks.uiuc.edu/Research/vmd/.

22 (*a*) M. Hennum, H. Fliegl, L.-L. Gundersen and O. Eisenstein, *J. Org. Chem.*, 2014, **79**, 2514; (*b*) B. Castro, R. Chaudret, G. Ricci, M. Kurz, P. Ochsenbein, G. Kretzschmar, V. Kraft, K. Rossen and O. Eisenstein, *J. Org. Chem.*, 2014, **79**, 5939; (*c*) J.-P. Piquemal, J. Pilmé, O. Parisel, H. Gérard, I. Fourré, J. Bergès, C. Gourlaouen, A. De La Lande, M. C. Van Severen and B. Silvi, *Int. J. Quantum Chem.*, 2008, **108**, 1951; (*d*) R. Chaudret, G. A. Cisneros, O. Parisel and J.-P. Piquemal, *Chem. – Eur. J.*, 2011, **17**, 2833; (*e*) P. Wu, R. Chaudret, X. Hu and W. T. Yang, *J. Chem. Theory Comput.*, 2013, **9**, 2226; (*f*) M. Alonso, P. Geerlings and F. De Proft, *Chem. – Eur. J.*, 2013, **19**, 1617.

23 L. R. Domingo, *J. Org. Chem.*, 2001, **66**, 3211.

24 (*a*) A. Arrieta and F. P. Cossío, *J. Org. Chem.*, 2001, **66**, 6178; (*b*) C. S. Wannere, A. Paul, R. Herges, K. N. Houk, H. F. Schaefer III and P. v. R. Schleyer, *J. Comput. Chem.*, 2007, **28**, 344.

25 G. Bott, L. D. Field and S. Sternhell, *J. Am. Chem. Soc.*, 1980, **102**, 5618.

26 K. Alder, *Experientia, Suppl. II*, 1955, 86; J. Sauer, *Angew. Chem., Int. Ed. Engl.*, 1967, **6**, 16 and references therein. O. Eisenstein and N. T. Anh, *Tetrahedron Lett.*, 1971, 1191; R. Sustmann, *Tetrahedron Lett.*, 1971, 2721; O. Eisenstein and N. T. Anh, *Bull. Soc. Chim. Fr.*, 1973, 2721; O. Eisenstein and N. T. Anh, *Bull. Soc. Chim. Fr.*, 1973, 2723; N. T. Anh, E. Canadell and O. Eisenstein, *Tetrahedron*, 1978, **34**, 2283. See also K. N. Houk, J. Gonzàlez and Y. Li, *Acc. Chem. Res.*, 1995, **28**, 81; K. N. Houk, Y. Li and J. D. Evanseck, *Angew. Chem., Int. Ed. Engl.*, 1992, **31**, 682.

27 (*a*) T. Steiner, *Angew. Chem., Int. Ed.*, 2002, **41**, 48; (*b*) O. Takahashi, Y. Kohno and M. Nishio, *Chem. Rev.*, 2010, **110**, 6049; (*c*) M. J. Nishio, *Phys. Chem. Chem. Phys.*, 2011, **13**, 1387; (*d*) M. J. Nishio, *J. Mol. Struct.*, 2012, **1018**, 2. The web-site http://www.tim.hi-ho.ne.jp/dionisio provides up-to-date information on CH–π interactions.